AEROELASTIC INSTABILITY OF PLATE SUBJECT TO NORMAL JET

M. Antoine, P. Hémon, E. de Langre

LadHyX, Ecole Polytechnique – CNRS, F-91128 PALAISEAU, France

ABSTRACT

A flexible sheet subject to a normal impinging air jet can oscillate. We present a simple experiment that shows that added damping generated by the jet is responsible for this aeroelastic instability. The cases of planar jet and circular jet are studied. A model is presented to describe this instability and the results agree well with the experimental observations. The nozzle geometry is found to be a dominant parameter that drives the critical distance between the jet and the sheet, under which the instability develops.

1. INTRODUCTION

We deal with the problem of a flexible sheet which can oscillate at low frequency when it is subject to a normal impinging air jet. This configuration arises in several industrial processes of metal sheet production where series of perpendicular jets are used as cooling or dryer devices over long rectangular thin sheet (Renard et al 2003). Most of the time, the amplitudes of the oscillations are limited mechanically due to the jet nozzle, leading to violent contact between the plate and the nozzle, which is not acceptable in practice.

Preliminary studies based on observations have led to eliminate a mechanism of excitation caused by the jet instabilities, due to the large differences in frequencies. Moreover, a broadband turbulent excitation is not sufficient to explain the large, and mainly sudden amplitudes of oscillations that are observed in field tests.

An aeroelastic instability is therefore suspected to be responsible for these oscillations. In this paper we deal with a simplified configuration where the sheet is replaced by a rigid plate and the flexibility is provided by springs, as shown Figure 1.

The plate motion is restricted to a translational motion parallel to the jet axis which is set at the distance H from the plate surface. The plate can oscillate along the z axis. The objective of this paper is to propose a validated modelling of the fluid-structure interaction mechanism observed in the experiments.
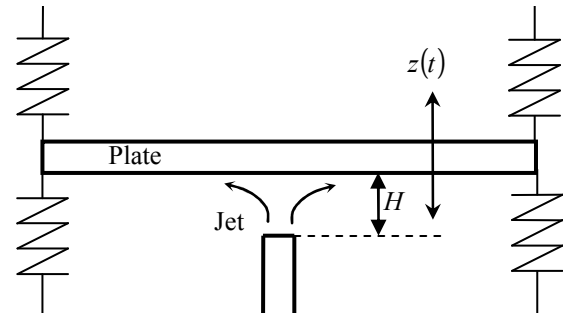
Figure 1: *Jet-plate system.*

2. EXPERIMENTAL TECHNIQUES

In the experiment, two different jet nozzles, circular or rectangular, blow an airstream on a rigid plate which is mounted flexibly with linear springs, as sketched in figures 2 and 3. For the rectangular nozzle, the span-wise dimension L is much larger than the jet thickness d so that the jet flow is assumed to be planar. The distance H can be varied accurately using a micrometric displacement rail, see figure 4. The plate motion is recorded with laser displacement sensors and standard signal analysis is performed to extract the added damping of the plate under the action of the jet. The experimental setup design leads to a very low structural damping in the absence of flow so that it does not perturb the added damping measurements.
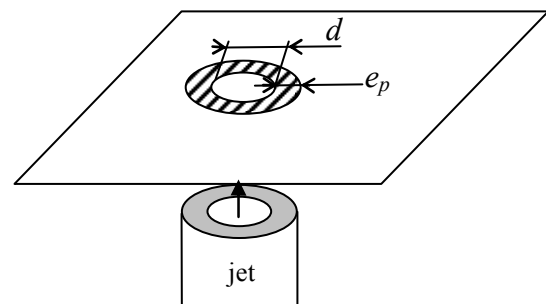
Figure 2: *Geometric parameters for the circular jet.*

All the signals are connected to an acquisition system PAK provided by Mueller-BBM. It consists mainly of a 24 bits and 8 channels acquisition card

and a signal processing software. Static calibration is first performed in order to estimate the global stiffness of the system by using calibrated weights. Then the frequency is measured by Fourier analysis.
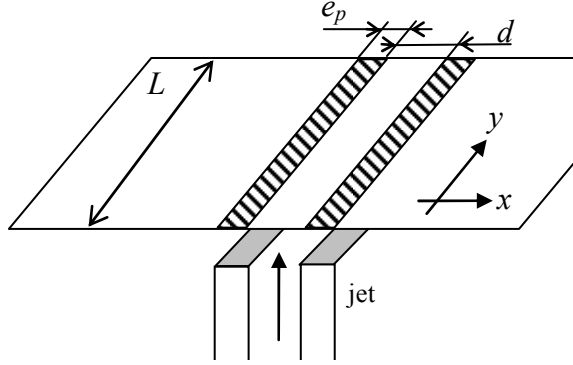
Figure 3: *Geometric parameters for the plane jet.*

The jet flow is produced with domestic compressed air circuit. The output velocity is controlled with a manometer connected to the upstream circuit. The effect of the upstream circuit on the oscillations of the plate (tube length, volume of pressure chamber) has been investigated and no influence has been detected.

Few measurements with hot wire have shown that the velocity at the outlet of the jet can be well estimated with Bernoulli equation, starting from pressure measurements in the chamber upstream the jet.
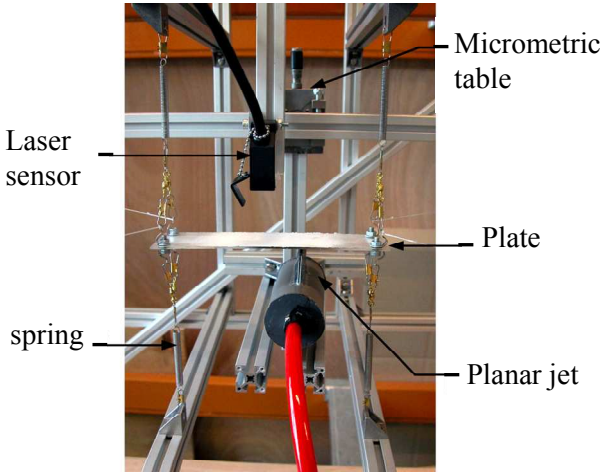
Figure 4: *View of the experimental setup.*

3. EXPERIMENTAL RESULTS

Below a critical distance of the nozzle, the plate undergoes self-sustained oscillations. Observations of the plate motion, especially the growth rate in the unstable case, leads us to explore the added

damping generated by the jet. The experimental results are presented in Figures 5 and 6 for the circular and plane jet respectively. Filled circles are measured during amplitude growing of the plate motion, in the unstable region. These measurements show that this aeroelastic instability arises by decreasing damping, the critical distance being consistant with the sudden decrease of the damping. We present now a modelling for this behaviour.
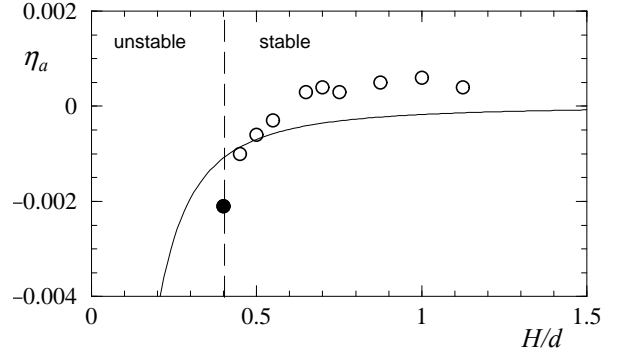
Figure 5: *Comparison of measurements (○ stable, ● unstable) and predictions (—) of the added damping for the circular jet.*
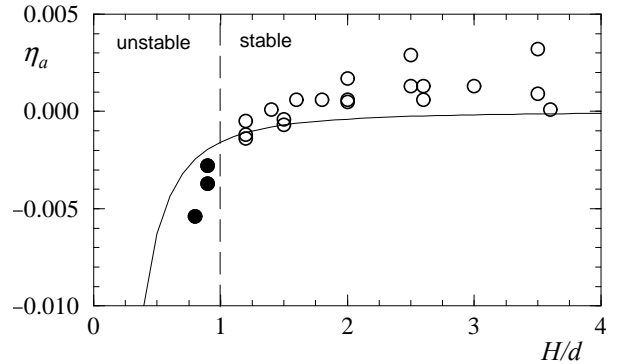
Figure 6: *Comparison of measurements (○ stable, ● unstable) and predictions (—) of the added damping for the plane jet.*

4. MODELLING EQUATIONS

The equation of motion for the plate is given in equation (1) where m is the mass, c the structural damping, k the stiffness provided by the springs and F the impact force of the jet which is assumed to depend on the plate motion through its position z, its velocity $\dot{z}$ and its acceleration $\ddot{z}$,

$$m\ddot{z} + c\dot{z} + k z = F(z, \dot{z}, \ddot{z}). \qquad (1)$$

When the distance H is small, this force results from the leakage flow confined between the jet

nozzle and the plate (Porcher & de Langre 1997; Païdoussis 2004). In order to estimate it we use the model of Porcher and de Langre (1997) that deals with the pressure variations generated by the plate motion. The linearized model assumes that the pressure P and the flow velocity U are decomposed in a mean component and a fluctuating component, so that

$$P(x,t) = \overline{P} + p(x,t); \quad U(x,t) = \overline{U} + u(x,t). \quad (2)$$

A volume is defined between the jet nozzle and the plate, as shown in Figure 7, where the inlet denotes A and the outlet B. The pressure is P_{ext} outside. At the inlet A we assume that there is no velocity fluctuation and that the Bernoulli equation for pressure recovery at the outlet B remains valid when the plate oscillates. Assuming incompressible flow and neglecting viscosity, we apply the decomposition (2) to the Euler equations

$$div\, U = 0$$
$$\rho \frac{dU}{dt} = -grad\, P \quad (3)$$

which leads to the conservation equations (4) at order 0 and 1, with the corresponding boundary conditions. Space and time derivatives are denoted by primes and dots respectively.

Order 0 : $\quad \overline{U}' = 0; \quad \overline{P}' + \rho \overline{U} u' = 0; \quad$ (4a)

with $\quad U_A = \overline{U}_A; \quad P_{ext} = P_B + \frac{1}{2}\rho U_B^2$

Order 1 : $\quad H u' - \dot{z} = 0; \quad p' + \rho \dot{u} + \rho \overline{U} u' = 0 \quad$ (4b)

with $\quad u_A = 0; \quad p_B + \rho u_B \overline{U}_B = 0$.
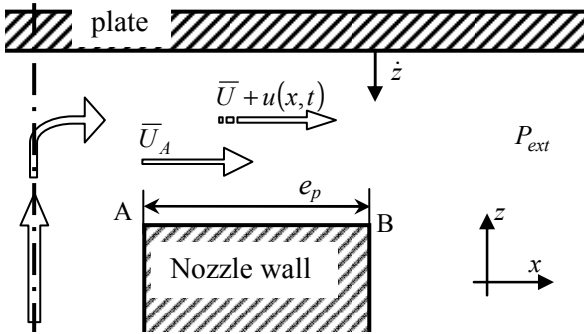
Figure 7: *Detailed sketch of the space between nozzle and plate.*

This set of equations allows to derive the pressure p along the coordinate x, equation (5).

$$u(x,t) = \frac{x}{H}\dot{z}$$

$$p(x,t) = -\rho U_A \frac{x}{H}\dot{z} - \frac{\rho}{2H}\left(x^2 - e_p^2\right)\ddot{z} \quad (5)$$

It can be integrated on the jet nozzle wall (AB) to give the force acting on the oscillating plate (6).

$$F(\dot{z},\ddot{z}) = \int_A^B p(x,t)dx = -\eta_a \,\dot{z} - m_{aj}\,\ddot{z} \quad (6)$$

This force, which is induced by the plate motion, includes an added mass term m_{aj} due to confinement (de Langre 2002) and an added damping term η_a that is responsible of the plate instability when it becomes negative.

Estimation of this added mass, due to the nozzle walls, is found to be negligible by comparison with the added mass due to ambient air surrounding the plate. If we assume that the plate has a dimension $a.b$ the added mass m_a for such configuration was given by Gibert (1994) and Blevins (1990).

$$m_a = \pi \rho_{air} \frac{a^2 b}{4} \frac{1}{1 + a/b} \quad \left(\text{with } b \rangle a\right). \quad (7)$$

Application of this formula to the case of very thin sheet, or plate, shows that added mass is comparable to the mass of the plate, and that it must be taken into account for a correct modelling of such a system.

5. RESULTS AND VALIDATION

The added damping η_a is now calculated for the different jet geometries. The resulting expressions are given in (8a) and (8b) for circular and plane jets respectively.

$$\eta_a^{circ} = -\frac{\pi \rho U_A \left(\left(d/2 + e_p\right)^3 - \left(d/2\right)^3\right)}{3H\sqrt{km}} \quad (8a)$$

$$\eta_a^{plan} = -\frac{\rho U_A L e_p^2}{2H\sqrt{km}} \quad (8b)$$

The comparisons between predictions and measurements of the added damping are presented figures 5 and 6 for the circular and plane jets respectively, with the distance H as a parameter. Agreement between predictions and measurements is good, considering the simplicity of the model. Moreover, although the nozzle geometry is taken into account, this model does not require any empirical parameters to be set, which is of great

interest in practical applications.

It must be noticed that the air velocity involved in the formula is the velocity U_A at the entrance of the confined volume between nozzle walls and the plate. It is estimated starting from the velocity at the outlet of the jet U_j, see figure 8, and by flow rate conservation law for the circular and the planar jets. Resulting expressions are

$$U_A = U_j \frac{d^2}{4 e_p^2 + 2 d \, e_p}, \qquad (9a)$$

$$U_A = U_j \frac{d}{2 \, e_p}, \qquad (9b)$$

for the circular jet and planar jet respectively.
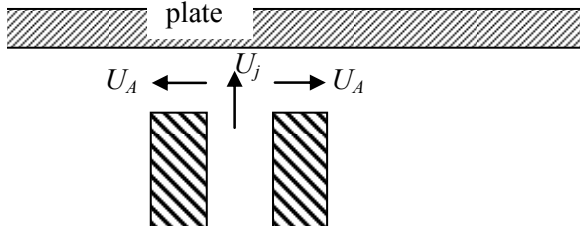
Figure 8: *Velocities between nozzle and plate.*

Improvement of the model can be performed by adding the added damping induced by the velocity gradient in the direction of the jet (Hémon 2006). However, this is expected to improve the agreement between experiments and predictions only for large distance H, and will not modify the critical distance under which plate motion is unstable.

6. NOMENCLATURE

c structural damping
d jet diameter or thickness (m)
e_p nozzle thickness (m)
F transverse force (N)
H distance between nozzle and plate (m)
H_c critical distance (m)
k stiffness (N/m)
L planar jet width (m)
m mass involved in the vertical motion (kg)
P pressure (Pa)
U wind velocity (m/s)
x tangential coordinate (m)
z vertical displacement (m)
η_a reduced added damping (%)

7. REFERENCES

Blevins, R.D. 1990, Flow-Induced Vibrations. Van Nostrand Reinhold, New York.

de Langre, E., 2002, Fluides et Solides. Editions de l'Ecole Polytechnique.

Gibert, R.J., 1994, Vibrations des structures : interactions avec les fluides, sources d'excitation aléatoires. Collection de la DER d'EDF, Eyrolles, Paris.

Hémon, P., 2006, Vibrations des structures couplées avec le vent. Editions de l'Ecole Polytechnique.

Païdoussis, M. P., 2004, Fluid-structure interactions, Slender structures and Axial flow, volume 2, Elsevier, Amsterdam.

Porcher, G., de Langre, E., 1997, A friction-based model for fluidelastic forces induced by axial flow, in: 4th International Symposium on Fluid-structure interaction, Aeroelasticity, Flow-induced vibration and noise, ASME, Volume II, 67-74.

Renard, M., Gouriet, J.B., Planquart, P., van Beeck, J., Buchlin, J.M., 2003, Rapid cooling in continuous annealing and galvanizing lines, *La revue de métallurgie*, juillet-août, 751-756.